Pergamon

0038-1101(93)E0134-M

Solid-State Electronics Vol. 37, No. 10, pp. 1739–1751, 1994
Copyright © 1994 Elsevier Science Ltd
Printed in Great Britain. All rights reserved
0038-1101/94 $7.00 + 0.00

VERY-LOW-FREQUENCY RESONANCE OF MOSFET AMPLIFIER PARAMETERS

O. L. YAKYMAKHA and Y. M. KALNIBOLOTSKIJ

Laboratory of Electron Device Modelling, Department of Electro-Acoustic, 2330, Kyiv Polytechnic Institute, Peremogy Ave., 37, 252056 Kyiv, Ukraine

(Received 26 May 1993; in revised form 8 December 1993)

Abstract—Extensive investigations of frequency dependent MOSFET amplifier parameters are performed. For the first time gigantic very-low-frequency resonances are found with the bound values of the simple series resonant circuit $C_0 = 5.216 \times 10^{-7}$ F; $L_0 = 7.407 \times 10^{-2}$ H and $\omega_0 = 5088$ rad/s^{-1}. Analytical continuation of the MOSFET experimentally determined characteristic impedances $\rho(L_d)$ have given the wave vacuum value $\rho_0 = \sqrt{\mu_0/\epsilon_0}$ at the surface inductance zero value. Since the reactive MOSFET parameters L_d and C_d thicknesses were about the same order as the Compton wavelength of electron, the high values of L_0 and C_0 could be explained by the quantum properties of the Si–SiO_2 interface.

NOTATION

C_{gs}, C_{gd}, C_{ds}	terminal (stray) gate–source, gate–drain and drain–source capacitances, respectively (F)
C_{ch}	channel capacity (F)
C_0	bound value of surface resonant MOSFET capacitance (F)
E	supply source (V)
$\hbar$	$= h/2\pi$ reduced Planck's constant (Js)
I	current (A)
K_u	voltage transmission factor
L	inductance (H)
L_0	bound value of surface resonant MOSFET inductance (H)
l_y, l_z	length and width of MOSFET metallurgic channel (m)
M	voltage amplification factor
m	rest mass of electron (kg)
Q	quality factor
R	active resistance (Ω)
S	area (m^2)
T	absolute temperature (K)
$\mathbf{u}$	velocity (ms^{-1})
V, v	voltages (V)
Z	reactive resistance (Ω)
β	added parameter
δ	relative error
ϵ_0	permittivity of free space (Fm^{-1})
λ_x	surface capacity thickness (m)
λ_γ	helix step of induction coil (m)
μ_0	permeability of free space (Hm^{-1})
ν	frequency (Hz)
ρ	characteristic impedance (Ω)
ω	angular frequency (rad/s)

1. INTRODUCTION

It is well known that MOSFET frequency dependence is connected with parameters such as gate ($C_{g\Sigma}$), insulator (C_{0x}) and terminal (C_{gs}, C_{gd}, C_{ds}) capacitances. A MOS structure's gate capacitance dependence on the gate voltages (sc, C–V characteristics) is based on the classical Poisson's equation solved at the silicon surface in the case of thermodynamic equilibrium[1–3]. The frequency dependence of the gate capacitance $C_{g\Sigma}(\omega)$ is limited in the low region $\nu_L = (5\text{–}100)$ Hz by the speed of the recombination–generation process[1–3]. At the same time the MOS structure's C–V characteristics give useful information about the nature of fixed surface states in the Si–SiO_2 interface[4,5]. MOSFETs with non-zero drain voltage ($V_d \neq 0$) have C–V characteristics with saturation regions that conform to the theoretical prediction of multi-extrema structure based on the voltage-dependent bulk charge approximation method[6].

The insulator capacitance C_{0x} determines the MOSFET cut-off frequency[3,7–9]:

$$\nu_m = (1/2\pi)(\mathrm{d}I_d/\mathrm{d}Q_g)_{V_d} = S_g/2\pi C_{g\Sigma},$$

where

$$S_g = (\mathrm{d}I_d/\mathrm{d}V_g)_{V_d} \quad \text{and} \quad C_{g\Sigma} = (\mathrm{d}Q_g/\mathrm{d}V_g)_{V_d} \approx C_{0x}$$

are the MOSFET's transconductance and gate capacitance, respectively. Typical estimate for ν_m is higher than 2 GHz[8].

Intensive investigations of MOSFETs at the high frequencies showed the main influence of the terminal capacitances[10,11]. The real integrated MOS circuits with low values of transconductance have finite frequency about $\geqslant 2$ MHz where stray capacitances are dominating[8], but for improved MOS technology we have the value about $\leqslant 10$ GHz[9].

Today everybody considers that the MOSFETs' transconductances and consequently mobilities (μ_F) are frequency independent values. Fang and Fowler

[13,14], and Mellor[15] showed experimentally the equivalence of both a.c. and d.c. techniques for S_g measurements ($\leqslant 100$ kHz), but the a.c. method was generally used in [12–18] because of its simplicity and speed. It should be noted that the MOSFETs' transconductances[12–18] have been measured in the region below saturation (triode-like characteristics) and the MOSFETs had simple (rectangular or circular) channel topology.

This paper continues the consideration of the quantum phenomena in MOSFETs[19] with the comb channel topology. All investigations were made in the saturation region (pentode-like characteristics) at room temperature and higher. Firstly we wanted to control periodic bends of the static drain current–gate voltage I–V characteristics[19] using the alternative gate voltage $u_{gs}(\omega)$ at the very low frequency (VLF) band. But to our great surprise we found frequency dependence of the alternative output voltage $u_{ds}(\omega)$ at the VLF band with the load resistance values $R_L = (1\text{–}10)\,\text{k}\Omega$, that contradict the well known conception[12–18].

In the second section, the formal quadripole network MOSFET model is considered that allows the possibility to experimentally determine the internal MOSFET's parameters frequency dependence.

In the third section, the first-order approximation for the surface MOSFETs' reactive parameters is described. The experimental confirmation of the proposed model was done on serial Soviet MOSFETs (see Section 4). The main MOSFETs' amplifier parameters exhibit VLF resonance which may be explained by quantum mechanical considerations (see Section 5).

In the Appendix, the MOSFETs' VLF series resonant circuit is briefly described. Standard RLC considerations furnish an explanation of the main resonant parameters.

2. FORMAL ACTIVE QUADRIPOLE NETWORK MOSFETS' MODEL

From the engineering point of view the MOSFET can be represented as an active quadripole network (see Fig. 1). This formal black box model gives a simple method for the consideration of terminal capacitance. Since MOSFETs are nonlinear devices, y-matrix equations are only true for small changes of current and voltage.

Using Kirchhoff's laws to each mesh loop in the network of Fig. 1 we derive the MOSFETs' input dynamic conductance:

$$y_{11} = R_{gs}^{-1} + R_{ch}\omega^2 C_{ch}^2/[1 + (R_{ch}\omega C_{ch})^2] + j\omega\{C_{gs} + C_{gd} + C_{ch}/[1 + (R_{ch}\omega C_{ch})^2]\}. \quad (1)$$

This value is valid for the complete circuit shown in Fig. 1. The MOSFETs' input impedance is equal to the value $Z_{in} = y_{11}^{-1}$.

By analogy we can derive the MOSFETs' output dynamic conductance:

$$y_{22} = R_i^{-1} + j\omega(C_{ds} + C_{gd}). \quad (2)$$

This value is valid for the complete circuit shown in Fig. 1 at $R_{\Sigma g} = 0$. The MOSFETs' output impedance is equal to the value $Z_{out} = y_{22}^{-1}$.

The voltage transmission factor for MOSFET with common-source connection may be written through the y-matrix parameters as:

$$K_u = y_{\Sigma g}y_{21}/[y_{\Sigma g}(y_L + y_{22}) + y_L y_{11} + y_{11}y_{22} - y_{12}y_{21}], \quad (3)$$

where $y_{\Sigma g}$ is the sum of the output conductances of the low frequency generator ($v_{in\sim}$) and supply source ($v_{in=}$).

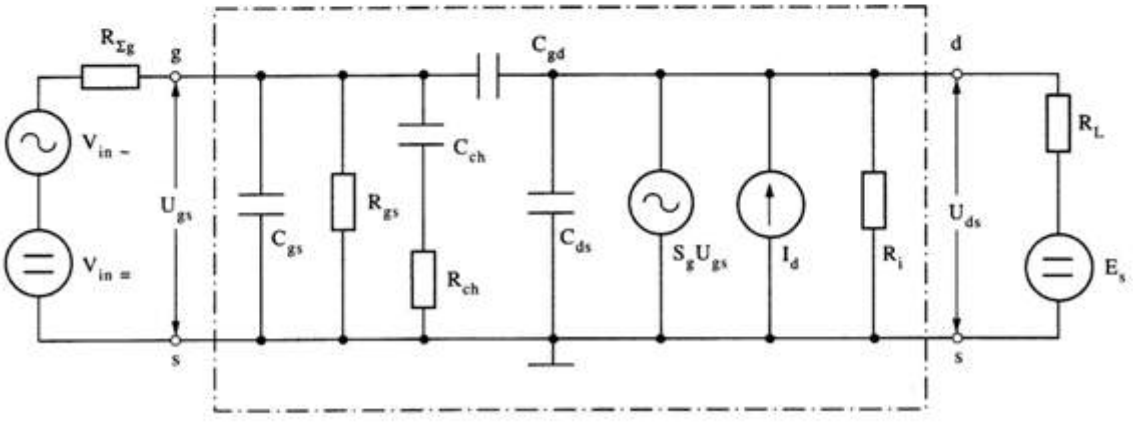

Fig. 1. The complete hybrid equivalent circuit with common-source connection. External elements are: $v_{in\sim}$—alternating voltage generator; $R_{\Sigma g}$—the total output resistance of input voltage sources; R_L—load resistance and E_s—supply source for drain. Internal elements are C_{gs}, C_{ch}, C_{gd} and C_{ds}—gate–source, channel, gate–drain and drain–source capacitances respectively; R_{gs}, R_{ch} and R_i—input, channel and differential resistances of MOSFET; $S_g \times u_{gs}$—the generator of output alternating current and $I_d(u_{gs})$—constant current source.

The influence of stray capacitance is negligibly small at the VLF band and we can approximate conductances in the simple forms:

$$y_{\Sigma g} = R_{\Sigma g}^{-1}; \quad y_L = R_L^{-1}; \quad y_{11} = R_{gs}^{-1}$$
$$y_{12} = 0; \quad y_{21} = S_g; \quad y_{22} = R_i^{-1}. \tag{4}$$

Inserting the values (4) into eqn (3) yields, for the low frequency:

$$K_u(\omega) = \{S_g(\omega) R_L R_i(\omega)/[R_L + R_i(\omega)]\} \times \{R_{gs}/[R_{gs} + R_{\Sigma g}]\}, \tag{5}$$

where $R_{gs} \gg R_{\Sigma g}$. Note that the second multiplier in eqn (5) can be neglected.

Equation (5) gives two boundary cases for the voltage transmission factor (VTF):

$$K_u(\omega) \approx \begin{cases} M_g(\omega), & \text{at } R_L \gg R_i(\omega) \\ R_L S_g(\omega), & \text{at } R_L \ll R_i(\omega) \end{cases} \tag{6}$$

where $M_g(\omega) = R_i(\omega) \times S_g(\omega)$ is the MOSFET voltage amplification factor. Knowing the fixed load resistance R_L we can find out the internal MOSFET parameters R_i and M_g from eqn (6). Moreover, by alternating the small input signal's frequency, we can determine the internal MOSFET parameters frequency dependence $R_i(\omega)$ and $M_g(\omega)$ at the VLF band. Using some commutated load resistances (minimum two) we can measure the $K_u(\omega, R_{L1}) = K_1$ and $K_u(\omega, R_{L2}) = K_2$ for either load resistances. The typical common-source connection of MOSFET (see Fig. 2) gives the following values of:

$$K_1 = u_{ds.1}/u_{gs.1} = R_{L1} M_g/(R_{L1} + R_i)$$
$$K_2 = u_{ds.2}/u_{gs.2} = R_{L2} M_g/(R_{L2} + R_i).$$

Determination of the VTF and the differential MOSFET's resistance can be made at constant frequency, $\omega = 2\pi\nu$, and input voltage, u_{gs}, values:

$$M_g = (K_2 - \beta_{21} K_1)/(1 - \beta_{21}) \tag{7a}$$

$$R_i = (\beta_{21} R_{L2} - R_{L1})/(1 - \beta_{21}), \tag{7b}$$

where $\beta_{21} = K_2 R_{L1}/K_1 R_{L2}$ is a dimensionless parameter. The error of the differential resistance determination can be defined by equation:

$$\delta_R = \Delta R_i/R_i = \{|dR_i/dR_{L1}|\Delta R_{L1} + |dR_i/dR_{L2}|\Delta R_{L2} + |dR_i/dK_1|\Delta K_1 + |dR_i/dK_2|\Delta K_2\} \times R_i^{-1}, \tag{8}$$

where partial derivatives have been found from (7b). Practical estimation of eqn (8) can be made for the typical values of parameters: $R_{L1} = 6.410\ \text{k}\Omega$; $R_{L2} = 9.090\ \text{k}\Omega$; $\Delta R_L = 0.002\ \text{k}\Omega$; $K_2 = 3.18$; $K_1 = 2.88$; $\beta_{21} = 0.786$. The errors for the two load resistances have values $\delta_R(R_{L1}) = 0.14\%$ and $\delta_R(R_{L2}) = 0.08\%$. Alternating voltages u_{gs} and u_{ds} were measured by the digital voltmeter with accuracy about 0.2%. The above y-matrix method allows the possibility for experimental determination of $R_i(\omega)$, $M_g(\omega)$ and $S_g(\omega)$ frequency dependence, but the physical nature of this dependence is not explained.

3. MOSFET CHARACTERISTIC IMPEDANCE MODEL

In this section we consider the reactive parameters that are connected with the Si–SiO_2 interface. Note that these parameters cannot be derived from the classical Poisson's equation approach.

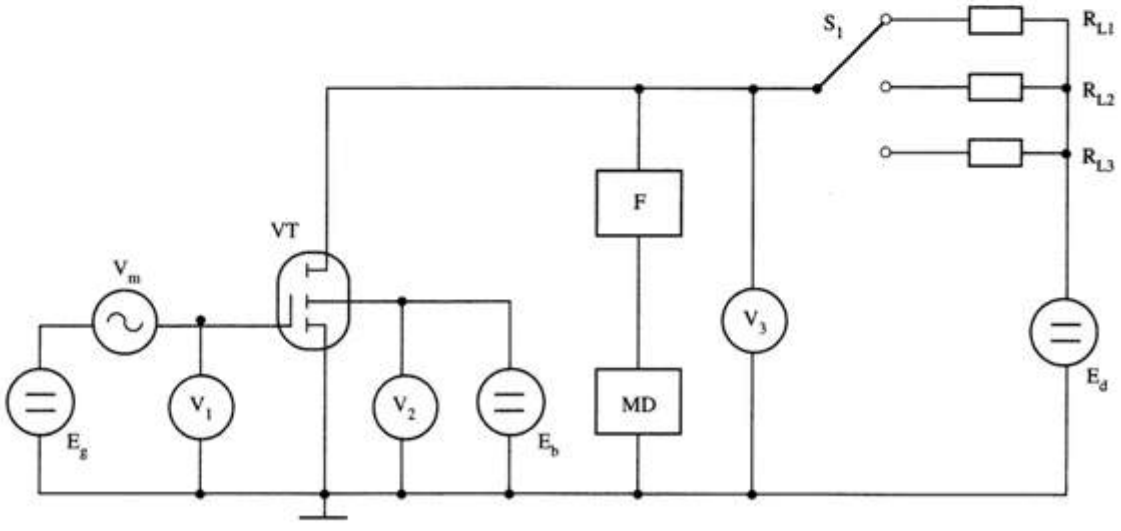

Fig. 2. The electric circuit for dynamics measurements of MOSFET. Used designations are as follows: VT—transistor, v_m—sound frequency generator; F—active VLF filter; MD—selective amplifier or digital voltmeter; S1—changeover switch; R_{Lj} ($j = 1, 2, 3, \ldots$)—load resistances; E_g, E_b and E_d—regulated supply sources for gate, bulk and drain electrodes respectively.

The planar surface MOSFET capacitance can be formally defined by:

$$C_d = S_{yz}\epsilon_0/\lambda_x, \tag{9}$$

where $S_{yz} = l_y l_z$ is the channel surface and λ_x is capacitance thickness (since λ_x is very small, then $\epsilon \approx 1$). It is evident that capacitance (9) cannot be tied with known MOSFET parameters such as channel or space charge capacitances, etc.

Analogically the planar surface MOSFET inductance can be formally defined by:

$$L_d = N^2 S_{xz}\mu_0/l_y, \tag{10}$$

where $S_{xz} = \lambda_x l_z$ is the channel cross section; $N = l_y/\lambda_y$ is the turn number of the planar induction coil; λ_y is the helix step of induction coil.

The characteristic impedance ρ_d [see eqn (A3) in Appendix] due to the surface MOSFET's reactive parameters (9) and (10) can be formally expanded in a Taylor series:

$$\rho_d = \sqrt{(L_0 + \Delta L)/(C_0 + \Delta C)} \approx \rho(L_0) + \{d\rho(L_0)/dL\}\Delta L + \{d\rho(C_0)/dC\}\Delta C = \rho_0[1 + 0.5(\Delta L/L_0 - \Delta C/C_0)] \tag{11a}$$

where

$$\rho_0 = \sqrt{L_0/C_0} = \sqrt{\mu_0/\epsilon_0} \approx 376.7302\,\Omega \tag{11b}$$

is the wave vacuum resistance, C_0 and L_0 are the bound values of surface resonant capacitance and inductance, respectively.

In the case when conditions:

$$L_d = L_0 + \Delta L; \quad C_d = C_0 + \Delta C; \quad \Delta L/L_0 + \Delta C/C_0 = -2 \tag{12}$$

are valid, then eqn (11a) can be rewritten in the form:

$$C_d(L_d) \approx L_d(C_0/L_0)(1 + L_d/L_0)^{-2}. \tag{13}$$

It is evident that capacitance function (13) has the maximum value $C_m = C_0/4$ at $L_m = L_0$. Inserting eqn (13) into eqn (A3) we find an approximation for the characteristic impedance:

$$\rho_d = \rho_0(1 + L_d/L_0), \tag{14}$$

that is confirmed by numerous experimental data (Fig. 11).

4. EXPERIMENTAL MOSFETS' FREQUENCY MEASUREMENTS

Production-type enhancement mode p-channel MOSFETs, КП301Б and КП304А, were used in this study. As is known, the КП301Б has the following values of the internal parameters: $l_y = 25\,\mu$m, $l_z = 2.2$ mm, $S_{g=} = (1\text{–}2.6)$ mA/V and $C_{gs} = 3.5$ pF, $C_{gd} = 1$ pF, $C_{ds} = 3.5$ pF which has been measured at $\nu = 1 \times 10^7$ Hz (see p. 578 in Ref. [20]), and the КП304А has the values: $l_y = 30\,\mu$m, $l_z = 4.6$ mm, $S_{g=} = 4$ mA/V and $C_{gS} = 9$ pF, $C_{gd} = 2$ pF, $C_{ds} = 6$ pF which have been measured at $\nu = 1 \times 10^6$ Hz (see p. 587 in Ref. [20]). Since $l_z/l_y \gg 1$, therefore, these transistors have the comb channel geometry shown in Fig. 3. The frequency dependence of the MOSFETs' amplifier parameters was measured by digital voltmeters with alternating current errors $\leqslant 0.1\%$ (see installation in Fig. 2). The input (u_{gs}) and output (u_{ds}) alternating voltages were measured twice for two different load resistor (R_L) values. The majority of experimental data were recorded at room temperatures, but in some cases we used a higher temperature (420 K) to find the resonance parameter's temperature dependence.

For MOSFET operation in the saturation region ($V_d \geqslant V_g - V_T$) the simple first-order theory[19] gives approximations:

$$I_d = I_g + I_{dif}, \tag{15a}$$

where

$$I_g = 0.5B_0(V_g - V_T)^2 \tag{15b}$$

is the generative (saturation) part of drain current [7,8,15], and:

$$I_{dif} = \gamma(V_g - V_T^*)V_d = S_{i=} \times V_d \tag{15c}$$

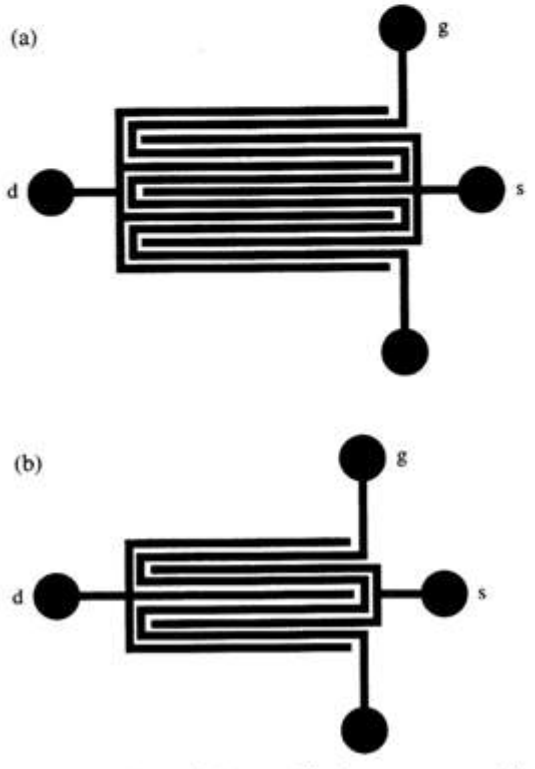

Fig. 3. Top view of the metallization geometry of the MOSFETs: КП304А (a) and КП301Б (b). (Not to scale.)

is the differential part of drain current that considers the non-zero value of saturation conductance ($S_{i\infty} \neq 0$), B_0 is the MOSFET's gain factor, V_T the standard threshold voltage (for generative current), V_T^* the fictitious threshold voltage (for differential drain current) and γ is the gain factor for differential drain current. Since eqns (15) contain the drain voltage that can vary from the zero value (Reddi and Sah channel length modulation model considers the case $V_d \geqslant V_{ds} = V_g - V_T$[21]), therefore the generative current corresponds to the "zero value of drain voltage" too. Such definition simplifies the experimental determination of the saturation drain current (I_g) since we should not measure the saturation drain voltage (V_{ds}). The unsaturated region of drain current:

$$I_d = [(V_g - V_T)V_d - 0.5V_d^2] + V_d S_{i\infty}$$

that considers $I_d = 0$ at $V_d = 0$ is beyond the scope of this work.

Simple approximations (15) allow the possibility to experimentally determine the threshold voltage by relationship:

$$\kappa = I_g/S_{gs} = 0.5(V_g - V_T), \tag{16a}$$

where $S_{gs} = (dI_g/dV_g)_{V_d}$ is the generative part of saturation transconductance, and Early voltage[22]:

$$V_{E\infty} = -I_g S_{i\infty}^{-1}, \tag{16b}$$

that is obtained using the condition $I_d = 0$.

Typical experimental data for d.c. measurements of the КП304А, N3 are shown in Fig. 4. The straight-line portion of the $\sqrt{I_g}$ vs V_g plot implies the constant values for gain factor and threshold voltage: $B_0 = 1.73$ mA/V^2, $V_T = -2.95$ V for $T = 293$ K and $B_0 = 0.786$ mA/V^2, $V_T = -2.47$ V for $T = 420$ K [see Fig. 3(a)]. As can be seen from Fig. 4(b) the saturation conductance is a linear function on gate voltage at $-V_g \geqslant 3.5$ V (for $T = 293$ K) and at $-V_g \geqslant 3.7$ V (for $T = 420$ K). The parameters of approximation (15c) can be determined from the data presented in Fig. 4(b) for the two regions of gate voltage: $\gamma_1 = 31\ \mu$S/V, $V_{T1}^* = -3.0$ V at $-V_g \leqslant 3.4$ V; $\gamma_2 = 58.4\ \mu$S/V, $V_{T2}^* = -3.2$ V at $-V_g > 3.4$ V for $T = 293$ K, and $\gamma_1 = 37.8\ \mu$S/V, $V_{T1}^* = -2.85$ V at $-V_g \leqslant 3.7$ V, $\gamma_2 = 55.2\ \mu$S/V, $V_{T2}^* = -3.10$ V at $-V_g > 3.7$ V for $T = 420$ K.

For the case when the small a.c. signal is applied to the gate of the MOSFET the drain current in the saturation region can be given by:

$$I_{dw} = I_{gw} + S_{iw} \times V_d, \tag{17a}$$

where $S_{iw} = R_{iw}^{-1}$ is the dynamic saturation conductance and I_{gw} is the dynamic generative current [it corresponds to the static saturation current I_g in eqns (15)]. Knowing the values of S_{iw}, V_d and $I_{dw} = I_{d\infty}$ we can determine the I_{gw} by eqn (17a). Differentiating the drain current in eqn (17a) with respect to V_g we will obtain the total dynamic transconductance:

$$S_{gw} = dI_{dw}/dV_g = S_{gsw} + S_{gdw}, \tag{17b}$$

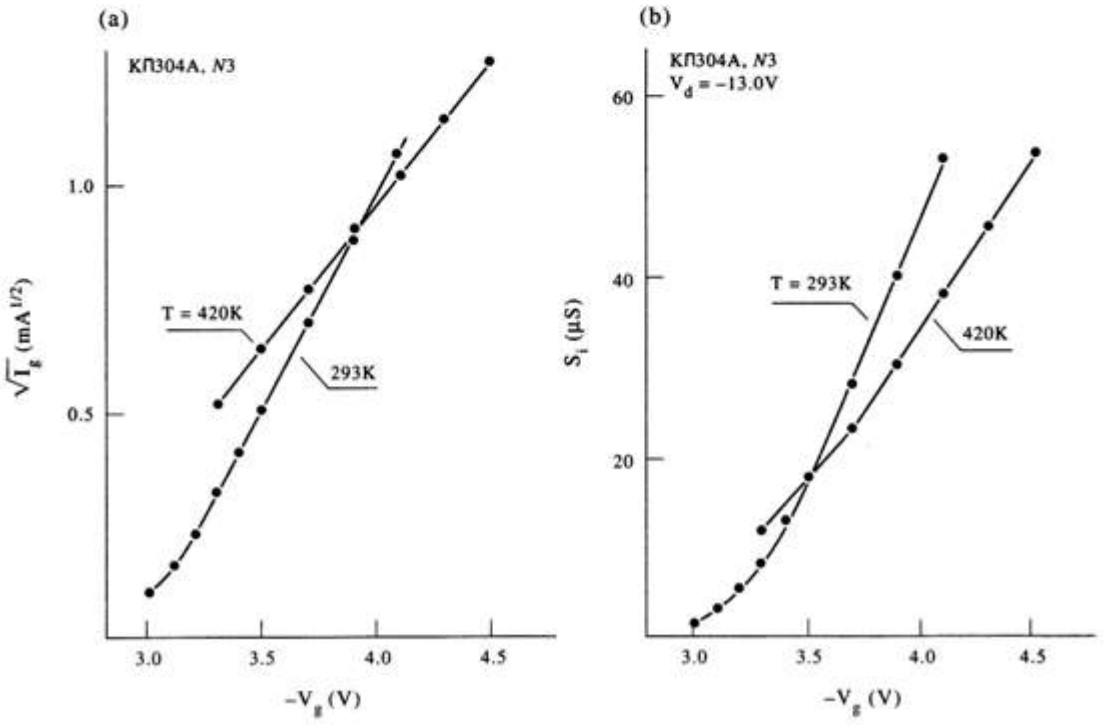

Fig. 4. The d.c. dependences of square root generative drain current (a) and differential conductance (b) on gate voltage at different temperatures for MOSFET КП304А, N3.

where $S_{gsw} = dI_{gw}/dV_g$ is the generative part of transconductance and $S_{gdw} = V_d(dS_{iw}/dV_g)$ is the differential part of transconductance.

By analogy to the expressions (16) we can derive the dynamic threshold voltage dependence:

$$\kappa_w = I_{gw}/S_{gw} = (I_{dw} - V_d S_{iw})/(S_{gw} - S_{gdw}) \quad (18a)$$

and dynamic Early voltage:

$$V_{Ew} = -I_{gw}/S_{iw}. \quad (18b)$$

Typical experimental data of the output voltage as a function of frequency are shown in Fig. 5 for MOSFET KП304A. It is seen that the output voltage $u_{ds}(\omega)$ is independent of frequency at $\nu \leqslant 0.5$ kHz and $\nu \geqslant 20$ kHz. In the range from 0.5 to 20 kHz the output voltage decreases by 4–5 times.

Table 1 shows a typical example of the theoretical treatment of the experimental data for MOSFET KП304A. The theoretical values for the dynamic output resistance, R_{iw}, and the voltage amplification factor, M_w, were calculated from eqns (7). The transconductance S_{gw}, was determined from the main device relation:

$$M_w = R_{iw} \times S_{gw}.$$

Dynamic generative current $I_{gw}(0) = I_{gw}(V_d) - V_d/R_{iw}$ (it corresponds to the saturation current in the Sah model[6]) was found in Table 1 by linear analytical extension of the saturation drain current $I_{gw}(V_d) = I_d(V_d)$ [where $I_d(V_d)$ is the static drain current at $V_d = -13.0$ V] to the zero drain voltage value ($V_d = 0$).

The results of the theoretical treatment of the experimental data are shown in Figs 6, 7 and 8 respectively for output resistance, generative current and transconductance as functions of frequency. All these functions have the resonance type dependence on frequency. It should be noted that dynamic resistance of MOSFET in the strong inversion is practically independent of gate and bulk voltages and temperature (see Fig. 6) at the frequency range $2\text{ kHz} \leqslant \nu \leqslant 10\text{ kHz}$. The minimal dynamic resistance value is $R_{iw} = (1.5\text{–}3.0)\,\text{k}\Omega$ in this frequency

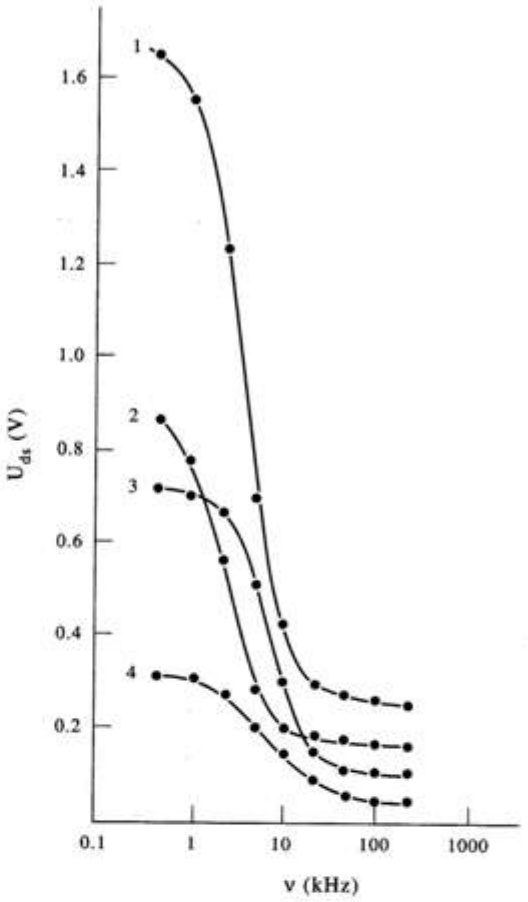

Fig. 5. Alternating output voltage as a function of frequency for MOSFET KП304A, N3 at $V_d = -13.0$ V; $T = 293$ K and $V_b = 0$. Curve 1 for $V_g = -4.1$ V; $R_L = 9.103$ kΩ; Curve 2 for $V_g = -3.3$ V; $R_L = 9.103$ kΩ; Curve 3 for $V_g = -4.1$ V; $R_L = 2.994$ kΩ; Curve 4 for $V_g = -3.3$ V; $R_L = 2.994$ kΩ.

Table 1. The results of experimental measurements and theoretical calculation of the main dynamic parameters of MOSFET KП304A, N3 at $T = 420$ K; $V_g = -3.3$ V; $V_b = 0$ V; $V_d = -13.0$ V and $u_{gi} = 95$ mV

ν (kHz)	u_{ds}, (mV) R_{L1}[a]	R_{L2}[b]	β_{21}	R_{iw} (kΩ)	M_w	S_{gw} (mS)	I_{gw} (mA)
0.5	863	316.5	0.8968	50.1	59.1	1.18	−0.040
1	769	310.4	0.8148	23.9	29.3	1.23	−0.324
2	571.5	289.7	0.6488	8.29	11.5	1.39	−1.348
3	444.3	264.8	0.5518	4.53	7.00	1.55	−2.651
4	359.6	238.7	0.4955	3.01	5.04	1.68	−4.105
6	266	190.4	0.4595	2.20	3.48	1.58	−5.692
8	226	157.3	0.4725	2.48	3.03	1.22	−5.024
10	205.4	130.8	0.5165	3.53	3.00	0.85	−3.461
12	196.7	113.3	0.5710	5.14	3.24	0.63	−2.311
14	189.8	98.7	0.6325	7.519	3.65	0.485	−1.509
16	185.8	88.9	0.6874	10.44	4.20	0.202	−1.025
18	183.7	81.8	0.7386	14.27	4.96	0.348	−0.691
20	181.7	76.1	0.7836	19.12	5.92	0.309	−0.460
50	177.4	62.7	0.9306	78.9	18.06	0.229	−0.055
100	177.3	61.8	0.9436	99.21	22.21	0.224	+0.089

[a] $R_{L1} = 9.103$ kΩ.
[b] $R_{L2} = 2.994$ kΩ.

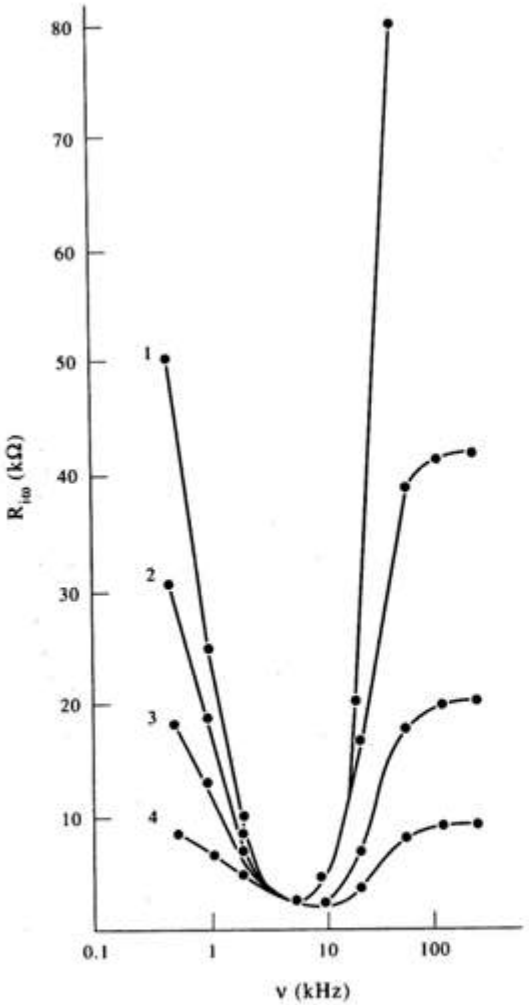

Fig. 6. The total output resistance as a function of frequency for MOSFET КП304А, N3 at $V_d = -13.0$ V. Curve 1 for $V_g = -3.3$ V; $V_b = 0$ V; $T = 293$ K; Curve 2 for $V_g = -3.8$ V; $V_b = +4.0$ V; $T = 293$ K; Curve 3 for $V_g = -4.3$ V; $V_b = -0$ V; $T = 420$ K; Curve 4 for $V_g = -4.8$ V; $V_b = +4.0$ V; $T = 293$ K.

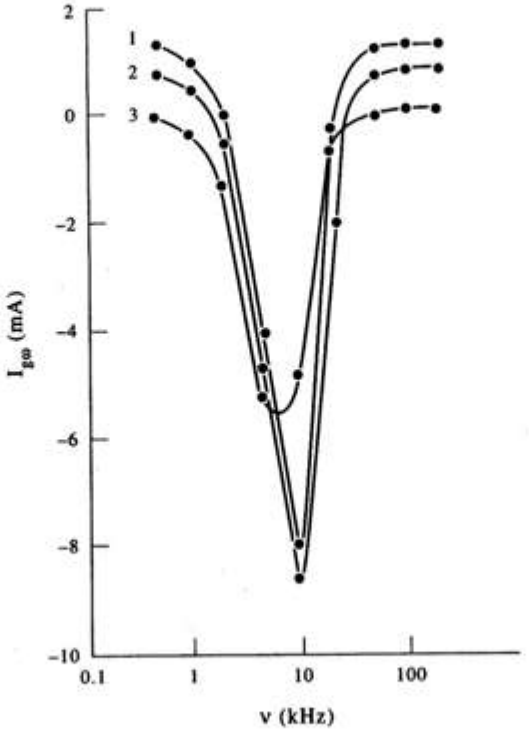

Fig. 7. Fictitious generative drain current as a function of frequency for MOSFET КП304А, N3 at $V_d = -13.0$ V. Curve 1 for $V_g = -4.3$ V; $V_b = 0$ V; $T = 420$ K; Curve 2 for $V_g = -4.8$ V; $V_b = +4.0$ V; $T = 293$ K; Curve 3 for $V_g = -3.3$ V; $V_b = 0$ V; $T = 293$ K.

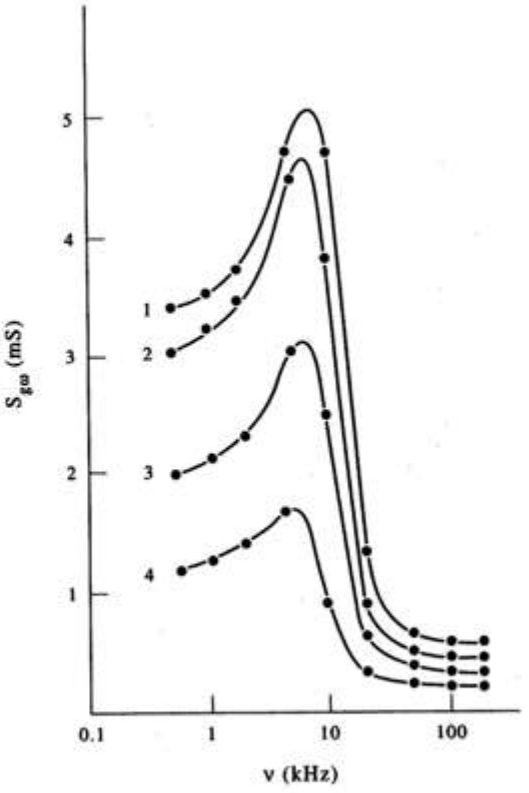

Fig. 8. The total transconductance as a function of frequency for MOSFET КП304А, N3 at $V_d = -13.0$ V. Curve 1 for $V_g = -4.8$ V; $V_b = +4.0$ V; $T = 293$ K; Curve 2 for $V_g = -4.1$ V; $V_b = 0$ V; $T = 293$ K; Curve 3 for $V_g = -4.3$ V; $V_b = 0$ V; $T = 420$ K; Curve 4 for $V_g = -3.3$ V; $V_b = 0$ V; $T = 293$ K.

band. The mean resonant frequency value is about $\nu_d(R) = 5.5$ kHz.

The minimal generative drain current value is a function of the gate voltage. It is practically independent of the bulk voltage and temperature (see Fig. 7). It follows from Fig. 7 that with the increase of gate voltages, the resonant frequency $\nu_d(I_{gw})$ increases in the range of 6–10 kHz.

MOSFET dynamic transconductance is a function of the gate and bulk voltages and temperature (see Fig. 8). The mean resonance frequency value is about $\nu_d(S) = 5.5$ kHz.

As can be seen from Fig. 9 the differential part of dynamic transconductance has the resonant type dependence on frequency. Moreover, its value $S_{gw} = 0.74$ mA/V is the same at low (< 1.0 kHz) and high (> 50 kHz) frequencies and equal to the static one $S_g = 0.76$ mA/V. The total dynamic transconductance is 6 times less in the range of high frequencies ($\geqslant 50$ kHz) than in the range of low frequencies ($\leqslant 1$ kHz). It is evident from Fig. 9 that the dynamic drain current cannot be represented by the simple approximation (15b) as the static drain current does.

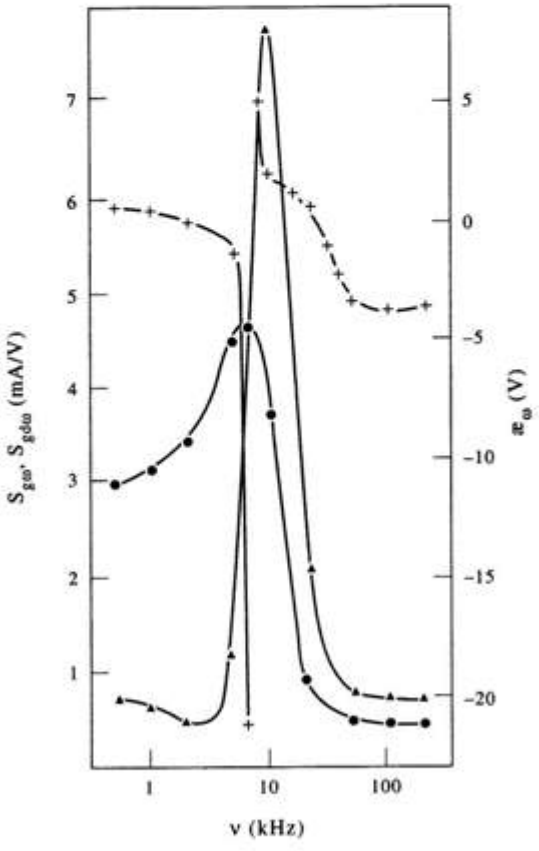

Fig. 9. MOSFET transconductances and gate threshold voltage as a function of frequency for KП304A, N3 at $V_g = -4.1$ V, $V_b = 0$ and $T = 293$ K. Designations: ●—S_{gw} (total dynamic transconductance); ▲—$S_{gdw} = V_d(R_{iw2} - R_{iw1})/(V_{g2} - V_{g1})$, where $V_{g1} = -3.3$ V, $V_{g2} = -4.1$ V and $V_d = -13.0$ V (differential part of dynamic transconductance); +—κ_w (gate threshold voltage).

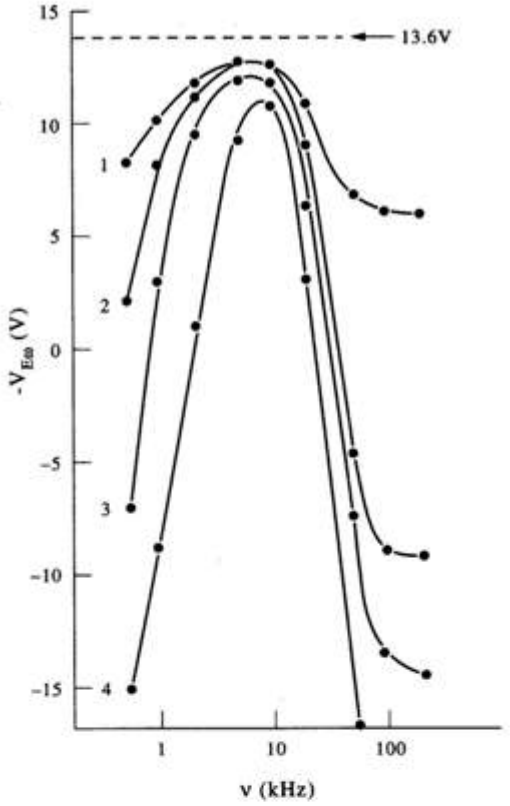

Fig. 10. The Early voltage as a function of frequency for MOSFET KП304A, N3 at $V_d = -13.0$ V and $T = 293$ K. Curve 1 for $V_g = -3.8$ V; $V_b = +4.0$ V; $V_E = -4.744$ V. Curve 2 for $V_g = -3.3$ V; $V_b = 0$ V; $V_E = 12.10$ V. Curve 3 for $V_g = -4.8$ V; $V_b = +4.0$ V; $V_E = 8.89$ V. Curve 4 for $V_g = -4.1$ V; $V_b = 0$ V; $V_E = 21.50$ V.

Actually, the dynamic threshold voltage (κ_w) has a break point near the resonant frequency $\nu_d = 7.5$ kHz and changes its sign from negative at $\nu < \nu_d$ to positive at $\nu > \nu_d$.

In the limits of channel-length modulation model [21], that considers differential resistance in the saturation region of drain voltages ($V_d \geqslant V_g - V_T$), we will have always the reverse sign of the Early voltage (V_E). Simple approximations (15) and (17) allow the direct sign of the Early voltage. Actually, Fig. 10 shows the dependence of dynamic Early voltage on frequency with direct and reverse signs of V_E. Note that direct sign of $V_E = -4.744$ V is seen for d.c. measurements at the reverse bulk voltage $V_b = +4.0$ V and small gate voltage $V_g = -3.8$ V. As can be seen from Fig. 10 the dynamic Early voltage has the resonant type dependence on frequency. Moreover, in the range near resonant frequency Early voltages have the direct sign and tend to the value 13.6 V that is close to the Bohr energy constant ($W_B = 13.6$ eV). This tendency is confirmed for every measured MOSFET.

Experimental determination of the main MOSFET parameters for the simple series resonant circuit has been made according to Appendix A. The first step

is to determine the resonant frequency $\nu_d = \omega_d/2\pi$ and active dynamic channel resistance $R_d = |\dot{Z}_{i\Sigma}(\omega_d)| = R_{i\Sigma}(\omega_d)$ from the experimental dependence $R_{i\omega}$ which is measured at V_g, V_b, $T = \text{const}$. The next step is to calculate the quality factor Q_d by eqn (A8) at the frequency ω_1 where the condition $R_{i\Sigma}(\omega_1) = \sqrt{2}R_d$ is valid. The characteristic impedunce $\rho_d = Q_d \times R_d$ may be calculated third and then the reactive parameters:

$$L_d = \rho_d/\omega_d, \quad C_d = (\rho_d \omega_d)^{-1} \tag{19}$$

can be calculated.

Results of the typical treatment of the experimental data for MOSFET in strong inversion are presented in Table 2. We can see the low value of the quality factor ($Q_d \leqslant 1$), but very high value of the inductance $L_d = (0.1\text{–}0.3)$ H and the capacitance $C_d = (8\text{–}10) \times 10^{-8}$ F. These high reactive values cannot be explained by the parasitic terminal reactive parameters.

The results of MOSFET characteristic impedance treatment as a function of inductance are shown in Fig. 11. The whole data for different MOSFET's type and their operation mode are presented in this figure. Characteristic impedance is a linear function of inductance (14). At $L_d = 0$ we will have the wave vacuum value $\rho_0 = \sqrt{\mu_0/\epsilon_0}$ for characteristic impedance and that is the most interesting result.

The relationship between MOSFET resonant surface capacitance and inductance is shown in Fig. 12. From this figure it is seen that approximation (13) fits well to the experimental data. The extremum parameters for the simple series resonant circuit $C_m = 1.304 \times 10^{-7}$ F and $L_m = L_0 = 7.407 \times 10^{-2}$ H are independent of MOSFET type or their operation mode.

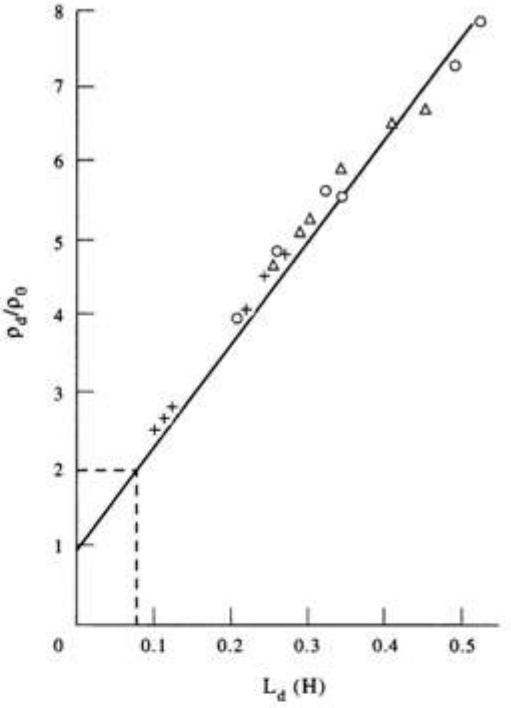

Fig. 11. Relationship between characteristics impedance and inductance of MOSFET in the strong inversion at different gate and bulk voltages and temperatures. Designations: +—КП304А, N3; ○—КП301Б, N11 and △—КП301Б, N15.

Experimental MOSFETs have the following geometry parameters:

$$S_{yz} = \begin{cases} l_y l_z = 1.38 \times 10^{-7}\,\text{m}^2, & \text{for КП304А} \\ l_y l_z = 5.5 \times 10^{-8}\,\text{m}^2, & \text{for КП301Б} \end{cases}$$

Table 2. The results of treatment of experimental data for MOSFETs in strong inversion at different gate and bulk voltages and temperatures

ν_d (kHz)	R_d (kΩ)	Q_d	ρ_d (kΩ)	L_d (H)	C_d (10^{-8} F)	Parameters
7.0	2.242	0.761	1.707	0.244	8.37	$V_g = -3.3$ V $V_b = 0$ V $T = 293$ K
8.5	1.34	0.786	1.053	0.124	11.2	$V_g = -4.1$ V $V_b = 0$ V $T = 293$ K
6.5	2.32	0.767	1.78	0.274	8.64	$V_g = -3.8$ V $V_b = +4.0$ V $T = 293$ K
9.5	1.20	0.806	0.967	0.102	10.9	$V_g = -4.8$ V $V_b = +4.0$ V $T = 293$ K
7.0	2.067	0.729	1.508	0.215	9.48	$V_g = -3.3$ V $V_b = 0$ V $T = 420$ K
8.5	1.32	0.748	0.987	0.116	11.9	$V_g = -4.3$ V $V_b = 0$ V $T = 420$ K

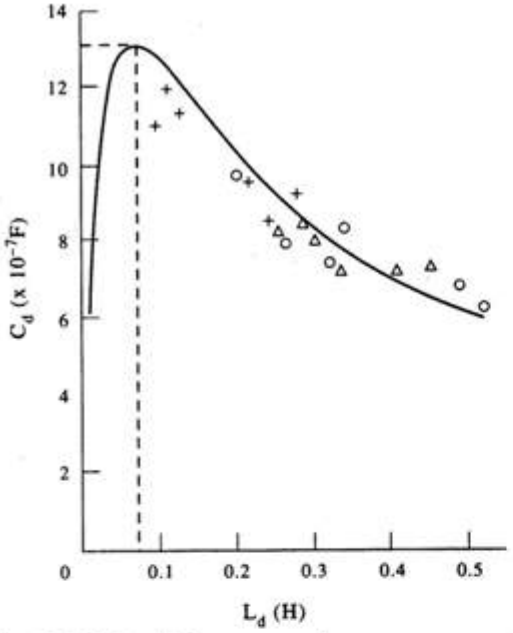

Fig. 12. Relationship between reactive parameters capacitance and inductance of MOSFET in the strong inversion at different gate and bulk voltages, and temperatures. Designations are the same as those in Fig. 7. Solid curve has been described by eqn (13) with $C_m = 1.304 \times 10^{-7}$ F and $L_m = 7.407 \times 10^{-2}$ H.

Using eqn (9) we can find the bound value for the capacitance thickness.

$$\lambda_{Cx} = \epsilon_0 S_{yz}/C_0 = \begin{cases} 2.34 \times 10^{-12}\,\text{m}, & \text{for КП304А} \\ 9.34 \times 10^{-13}\,\text{m}, & \text{for КП301Б}. \end{cases} \tag{20}$$

These values are the same order of magnitude as the Compton wavelength of electron $\lambda_0 = h/mc = 2.426 \times 10^{-12}$ m (where m is the rest mass of electron and c the velocity of light). In the same way, using eqn (10), we find the inductance thickness of the planar coil at $\lambda_y = \lambda_0$:

$$\lambda_{Lx} = L_0 \lambda_0^2/\mu_0 S_{yz} = \begin{cases} 2.511 \times 10^{-12}\,\text{m}, & \text{for КП304А} \\ 6.30 \times 10^{-12}\,\text{m}, & \text{for КП301В}. \end{cases} \tag{21}$$

From eqns (20) and (21) it can be seen that $\lambda_{Cx} \approx \lambda_{Lx}$ for the MOSFETs of КП304А type. Distinction λ_x for the MOSFETs of КП301Б type is caused by an approximate character of the model presented. In an exact quantum model it is necessary to take into account the active MOSFET surface, but not the metallurgic one (see Section 5). It is not so much the difference between λ_{Cx} and λ_{Lx} that is important but their closeness to the Compton wavelength of electron. That shows the existence of a stable quantum state at the Si–SiO_2 interface.

5. DISCUSSION

It is evident that the thickness parameters of the surface MOSFET's capacitance and inductance ($\lambda_x \approx \lambda_0$) show the quantum character of processes at the silicon surface. We can use the typical condition for quantization of velocity circulation[23]:

$$\oint (\mathbf{u}, \mathbf{dl}) = n \times h/m, \tag{22}$$

for the quantum system of the surface charges. This condition can be transformed for the MOSFET simple series resonant circuit:

$$n_0 \omega_0 S_0 = h/m, \tag{23}$$

where $n = 1$ and n_0 are digital values which consider the number of parallelly connected sheet area elements S_0. Since the reactive parameters C_0 and L_0 are known from experimental investigations, then we can find out the bound value for resonance frequency:

$$\omega_0 = (C_0 L_0)^{-1/2} = 5088\ \text{rad/s}.$$

Using eqn (23) we can derive the active area element, S_0, for the MOSFET surface:

$$S_{0a} = (h/m\omega_0) n_0^{-1}, \tag{24}$$

which value $S_{01} = 1.43 \times 10^{-7}$ m^2 at $n_0 = 1$ is close to the metallurgic surface for КП304А (for КП301Б we have $S_{yz} = S_{02} = 7.148 \times 10^{-8}$ m^2 at $n_0 = 2$). Now we can explain the difference $\lambda_{Cx} \neq \lambda_{Lx}$ for the КП301Б in the following way. As is known the parallel connection of capacitances gives:

$$C_{0\Sigma} = C_{01} + C_{02} = 2C_0 = \epsilon_0 S_{yz}/(0.5\lambda), \tag{25a}$$

where $C_{01} = C_{02} = \epsilon_0 S_{yz}/\lambda_{Cx}$ is considered. By analogy, the series connection of inductances gives:

$$L_{0\Sigma} = L_{01} + L_{02} = 2L_0 = (\mu_0 S_{yz}/\lambda_0^2)(2\lambda_{Lx}), \tag{25b}$$

where $L_{01} = L_{02} = (\mu_0 S_{yz}/\lambda_0^2)\lambda_{Lx}$ is considered. It is evident from eqns (25) that the simultaneous series connection of inductances and parallel connection of capacitances will give the same thickness value $\lambda_{Cx} = \lambda_{Lx} = \lambda_0$ and by 2 times fictitious increase of the metallurgic MOSFET's surface $S_{01} = 2S_{yz}$ (the case of the КП301Б). These considerations underline the quantum character of the above phenomenon since the parallel connection of capacitances in the classical case leads to the parallel connection of corresponding inductances.

Mesascopic quantum of the MOSFET's area element S_0 has ξ microscopic lattice area elements a^2:

$$\xi = S_{01}/a^2 = 4.848 \times 10^{11},$$

where $a = 5.431 \times 10^{-10}$ m is the silicon lattice constant.

The origin of the MOSFET mesascopic quantum such as the sheet area element S_0 and surface capacitance C_0 we can formally explain in the following way. Formal Bohr atomic capacitance can be defined by the approximation:

$$C_B = 4\pi\epsilon_0 a_B^2/\lambda_0 = 1.284 \times 10^{-19}\ \text{F},$$

where a_B is the radius of Bohr atom. Multiplying the value C_B on the number ξ of the lattice elementary area, we can find an estimation for the total capacitance of the silicon surface:

$$C^*_{\Sigma_s} = \xi C_B = S_0 C_B/a^2 = 6.225 \times 10^{-8}\ \text{F},$$

which value is the same order of magnitude as the experimentally determined capacitance C_0 ($C_0/C^*_{\Sigma_s} = 8.379$). The deviation between C_0 and $C^*_{\Sigma_s}$ could be caused by the dielectric permitivity constant (ϵ_m).

It follows that the MOSFET low frequency capacitance is connected with the Si–SiO_2 interface. Moreover, this capacitance is determined completely by the quantum processes that take place in the two-dimensional system formed by the surface lattice atoms (the first-order quantum model for Schottky effect that considers in detail the above phenomenon is presented in Appendix B).

6. CONCLUSION

The results presented in this paper may be summarized in the following way.

1. A simple quadripole network model has been developed for the MOSFETs' internal parameter determination.

2. A simple series resonance circuit model was proposed for explaining the MOSFETs' internal parameter frequency dependence in the VLF band.

3. A first-order theory of the surface MOSFETs' reactive parameters was proposed for explaining the VLF resonance.

4. It was found experimentally that the resonance character of most MOSFETs' internal parameters frequency dependence was in the VLF band.

5. High values of the MOSFETs' resonant capacitance and inductance are due to the small values of their dimensions (about Compton wavelength value).

6. It is shown that simple quantum consideration of MOSFETs' resonant dependence predicts mesascopic quantum for the surface sheet area element $S_0 = 1.43 \times 10^{-7}\ \text{m}^2$.

7. It was found that analytical extension of MOSFETs' impedances $\rho(L_d)$ gave the wave vacuum value $\rho_0 = \sqrt{\mu_0/\epsilon_0}$ at the $L_d = 0$.

REFERENCES

1. J. Torkel Wallmark and Harwich Johnson (Editors), *Field-Effect Transistors. Physics, Technology and Applications.* Prentice Hall, Englewood Cliffs, N.J. (1971). (Russian edn).
2. R. S. C. Cobbold, *Theory and Applications of Field-Effect Transistors.* Wiley-Interscience, New York (1970). (Russian edn 1975).
3. S. M. Sze, *Physics of Semiconductor Devices*, 2nd edn, p. 355. Wiley-Interscience, New York (1981). (Russian edn 1984 in two books).
4. B. E. Deal, A. S. Grove, E. H. Snow and C. T. Sah, *J. appl. Phys.* **35,** 2458 (1964).
5. B. E. Deal, A. S. Grove, C. T. Sah and E. H. Snow, *Solid-St. Electron.* **8,** 145 (1965).
6. C. T. Sah and H. C. Pao, *IEEE Trans. Electron Devices* **ED-13,** 393 (1966).
7. C. T. Sah, *IEEE Trans. Electron Devices* **ED-11,** 324 (1964).
8. R. H. Crawford, *MOSFET in Circuit Design*, p. 182. McGraw-Hill, New York (1967).
9. A. Blicher, *Field-effect and Bipolar Power Transistors.* Academic Press, New York (1981). (Russian edn 1986).
10. J. A. Gerst, *Solid-St. Electron.* **8,** 88 (1965).
11. J. A. Gerst and H. J. Nunnik, *Solid-St. Electron.* **8,** 769 (1965).
12. O. Leistiko, A. S. Grove and C. T. Sah, *IEEE Trans. Electron Devices* **ED-12,** 248 (1965).
13. F. F. Fang and A. B. Fowler, *Phys. Rev.* **13,** 619 (1968).
14. T. Ando, A. Fowler and F. Stern, *Rev. mod. Phys.* **54,** N2 (1982). (Russian edn 1985).
15. P. J. T. Mellor, *Proc. IEE* **118,** 1393 (1971).
16. C. T. Sah, T. H. Ning and L. L. Tschopp, *Surf. Sci.* **32,** 561 (1972).
17. G. Gibaudo, *J. Phys. C: Solid State Phys.* **19,** 767 (1986).
18. G. Gibaudo and F. Balestra, *Solid-St. Electron.* **31,** 105 (1988).
19. O. L. Yakymakha, *High Temperature Quantum Galvanomagnetic Effects in the Two-Dimensional Inversion Layers of MOS Transistors*, p. 91. Vyscha Shkola, Kyiv (1989). (in Russian).
20. *The Most Commonly Used Soviet Transistors* (Edited by B. L. Perelmann *et al.*), p. 656. Radio i Svyaz, Moscow (1981) (in Russian).
21. V. K. G. Reddi and C. T. Sah, *IEEE Trans. Electron Devices* **ED-12,** 139 (1965).
22. J. M. Early, *Proc. IRE* **40,** 1401 (1952).
23. S. J. Putterman, *Superfluid hydrodynamics.* North-Holland, Amsterdam (1974). (Russian edn 1978).
24. G. Arfken, *Mathematical Methods for Physicists.* Academic Press, New York. (Russian edn 1970).
25. D. Colman, R. T. Bate and J. P. Mize, *J. appl. Phys.* **39,** 1923 (1968).
26. A. P. Gnadinger and H. E. Talley, *Solid-St. Electron.* **13,** 1301 (1970).

APPENDIX A

Series Resonant Circuit Formal MOSFET VLF Resonance Model

Let us consider the simplest formal MOSFET VLF resonance model based on the series resonant circuit (see Fig. A1).

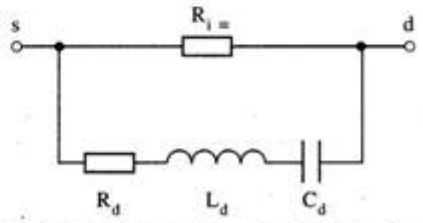

Fig. A1. Equivalent series resonant circuit for frequency dependent MOSFET's amplifier parameters.

It is evident that this model does not ascertain the physical nature of MOSFET parameters frequency dependence, but it is useful for estimation of VLF resonant parameters. The total differential impedance contains the frequency dependent and frequency independent parallel connected impedances:

$$\dot{Z}_{i\Sigma}^{-1} = R_{i\infty}^{-1} + \dot{Z}_{i\omega}^{-1},$$

where $\dot{Z}_{i\omega} = R_d + j(\omega L_d - 1/\omega C_d)$. The module of total differential impedance can be shown in the form:

$$|\dot{Z}_{i\Sigma}| = \sqrt{[(R_{i\infty} + R_d)R_d + (\omega L_d - 1/\omega C_d)^2]^2 + R_{i\infty}^2(\omega L_d - 1/\omega C_d)^2} \times R_{i\infty}/[(R_{i\infty} + R_d)^2 + (\omega L_d - 1/\omega C_d)^2]. \quad \text{(A1)}$$

Standard passive circuit's theory determines the main resonance parameters in the form:

$$\omega_d = (L_d C_d)^{-1/2} \quad \text{(A2)}$$

$$\rho_d = (L_d/C_d)^{1/2} \quad \text{(A3)}$$

$$Q_d = \rho_d/R_d, \quad \text{(A4)}$$

where ω_d is the resonance frequency; ρ_d is the characteristic impedance and Q_d is the quality factor.

The minimal value of differential resistance (A1) will be at the resonance frequency:

$$\min|\dot{Z}_{i\Sigma}| = R_d R_{i\infty}/(R_d + R_{i\infty}), \quad \text{(A5)}$$

and maximal value:

$$\max|\dot{Z}_{i\Sigma}| = R_{i\infty} \quad \text{(A6)}$$

will be at $\omega = 0$ and ∞.

For the simple series resonant (RLC) circuit (where $R_{i\infty} \approx \infty$) the module of output resistance can be written in the form:

$$|\dot{Z}_{i\Sigma}| = R_d\sqrt{1 + Q_d^2(\omega/\omega_d - \omega_d/\omega)^2}. \quad \text{(A7)}$$

Practical determination of resonance parameters can be made in the following way. Quasi-static differential resistance $R_{i\infty}$ have to be determined first from the static drain current characteristics. The resonance value of frequency ω_d will be determined second from the dynamic characteristics of $|\dot{Z}_{i\Sigma}(\omega)|$ at its minimum value (A5). Knowing the static resistance $R_{i\infty}$, we will find out R_d from eqn (A5). The quality factor (A4) can be determined from eqn (A7) by fixing the frequency at which $|\dot{Z}_{i\Sigma}|$ will have a value a few times less than the minimum ones:

$$Q_d = \sqrt{|\dot{Z}_{i\Sigma}|/R_d}/(\omega/\omega_d - \omega_d/\omega). \quad \text{(A8)}$$

The above simple series resonant circuit considerations will be used in the fourth section for formal investigation of the experimental resonance curves.

APPENDIX B

Schottky Effect

The classical Schottky effect can take place at the Si–SiO_2 interface with the mobile charge in the SiO_2:

$$Q_{ss}^* = qN_{ss}^*,$$

which take part of the metallic region into account and allow the possibility to introduce the reflection mechanism for charges with respect to a Si–SiO_2 plane of symmetry.

The Coulomb force of interaction for two reflected charges can be represented as[3]:

$$F_C = -q^2/4\pi\epsilon_0\epsilon_s(2x)^2. \quad \text{(B1)}$$

The work done by the field of an electron on another one to move it from infinity to the point x can be given [3] by:

$$A(x) = \int_{\infty}^{x} F_C\,dx = q^2/16\pi\epsilon_0\epsilon_s x. \quad \text{(B2)}$$

In the case of a constant electric field (E), the total energy of electron in the silicon will be:

$$W_\Sigma(x) = A(x) + U(x) = q^2/16\pi\epsilon_0\epsilon_s x + qxE. \quad \text{(B3)}$$

The extremum of the function (B3) may be obtained by differentiating it with respect to x:

$$dW_\Sigma/dx = -q^2/16\pi\epsilon_0\epsilon_s x_m + qE = 0,$$

from which the extremum point can be derived:

$$x_m = \sqrt{q/16\pi\epsilon_0\epsilon_s E}. \quad \text{(B4)}$$

Thus the classical Schottky effect consists of the reduction of the potential barrier at the Si–SiO_2 interface[3]:

$$\Delta\varphi = W_\Sigma(x_m)/q = \sqrt{qE/4\pi\epsilon_0\epsilon_s}. \quad \text{(B5)}$$

The quantum Schottky effect in the general case will be concerned with the Bohr atomic problem[24] that has the eigen-energy levels:

$$W_{Bn} = \hbar^2/2m(na_B)^2, \quad n = 1, 2, \ldots \quad \text{(B6)}$$

where a_B is the Bohr atomic radius, and with the Airy problem[25,26] that has the energy levels:

$$U_{An} = \eta_n(q\hbar E_n/\sqrt{2m})^{2/3}, \quad \text{(B7)}$$

where η_n is the roots of Airy function. Since atomic problem is a typical three-dimensional (3D) one and the Airy problem is a one-dimensional (1D) one, their compatible solution cannot be obtained in an analytical form. Thus, we will consider the first-order quasi-classical approximation to the above problem in the case of free motion of charges in the one dimension at the Si–SiO_2 interface.

As is known the quantum free motion of a particle can be represented by the flat wave:

$$\psi(x) \sim \exp(ikx),$$

where k is the wave vector magnitude, and kinetic energy:

$$W = (\hbar k)^2/2m. \quad \text{(B8a)}$$

In the case of the scattering centers the wave vector magnitude will satisfy a condition:

$$k(2x) = 1,$$

and therefore the one particle kinetic energy can be rewritten in the form:

$$W_{11} = \hbar^2/8mx^2. \quad \text{(B8b)}$$

Let us consider the one particle Schottky problem first for which the total energy can be represented as:

$$W_{11\Sigma}(x) = W_{11}(x) + U_{11}(x) = \hbar^2/8mx^2 + qxE. \quad \text{(B9)}$$

By analogy, using the differentiation of eqn (B9) with respect to x, we can derive the extremum point

$$x_{11m} = (\hbar^2/4mqE)^{1/3}, \quad \text{(B10)}$$

and Schottky potential barrier:

$$\Delta\varphi = W_{11\Sigma}(x_m)/q = (3/2q)(q\hbar E/2\sqrt{m})^{2/3}. \quad \text{(B11)}$$

The electric field (E) in eqn (B11) has only discrete values in the quantum case which can be derived by the following way. It is evident that quantum Bohr problem considers two particles interaction. Therefore for two particles we will have the kinetic energy (B8b) 2 times less than for one particle. The total energy in that case can be represented as:

$$W_{21\Sigma}(x) = W_{21}(x) + U_{21}(x) = \hbar^2/16mx^2 + qxE. \quad \text{(B12)}$$

By analogically, using differentiation of eqn (B12) we obtain the extremum point:

$$x_{12m} = 0.5(\hbar^2/mqE)^{1/3}, \quad \text{(B13a)}$$

kinetic energy:

$$W_{21}(x_m) = 2^{-5/3}(\hbar qE/\sqrt{2m})^{2/3} \quad \text{(B13b)}$$

and potential energy:

$$U_{21}(x_m) = 2^{-2/3}(\hbar qE/\sqrt{2m})^{2/3}. \quad \text{(B13c)}$$

Using the condition:

$$W_{21}(x_m) = W_{Bn} \quad \text{and} \quad U_{21}(x_m) = U_{A0},$$

we can derive the approximation for the electric field:

$$E_{0n} = (\sqrt{2m}/q\hbar)(\hbar^2/m\eta_s n^2 a_B^2)^{3/2} = 2^{3/2} n^{-3} \eta_0^{-3/2} E_B, \quad \text{(B14)}$$

where $E_B = \hbar^2/2mqa_B^3 = 2.5711 \times 10^{11}$ V/m, $\eta_0 = 2.33811$ is the zero value of the root of the Airy function (note that we consider only zero energy level for the Airy problem).

Substituting eqn (B15) into eqn (B11) we can derive the Schottky potential barrier:

$$\Delta\varphi_{0n} = (3/2q\eta_0 n^2)(q\hbar E_B/\sqrt{m})^{2/3} = 3a_B E_B/\eta_0 n^2 2^{2/3}. \quad \text{(B15)}$$

The space period of electric field can be derived from the Airy problem as:

$$x_{0n} = \eta_0(\hbar^2/2mqE_{0n})^{1/3} = na_B \eta_0^{3/2} 2^{-1/3}. \quad \text{(B16)}$$

Using the theorem of Gauss:

$$qN_{ss} = 2\epsilon_0 \epsilon_{ss} E_{0n}, \quad \text{(B17)}$$

we can calculate the surface density of states (N_{ss}). We shall be interested in the relationship:

$$N_{ss}/x_{0n}^{-2} = \epsilon_s \eta_0^{3/2}/2\pi n 2^{2/3}. \quad \text{(B18)}$$

The normalization procedure $N_{ss} = x_{0n}^{-2}$ allows the possibility to determine the relative permittivity for the surface:

$$\epsilon_{ss} = 2\pi n 2^{2/3} \eta_0^{-3/2} = 8.3693, \quad \text{(B19)}$$

for $n = 3$ in expressions (B6) and (B18). Since $x_{03} = 4.5048 \times 10^{-10}$ m $< a$(Si) at $n = 3$, than the 2D lattice determined by the density of states N_{ss} can be formed by electrons or holes (sc Wigner's lattice[14]). The electrons of the Wigner's lattice are interacted between themselves by plasmon mechanism. Using the energy condition:

$$q\Delta\varphi_{03} = \alpha^2 mc^2/3 \times 2^{5/3}\eta_0 = \hbar\omega_{ps} = \hbar\sqrt{q^2 N_{ss}/\epsilon_0 \epsilon_{ss} m a_{3D}},$$

we can derive the value a_{3D} of the 3D lattice constant:

$$a_{3D} = 32\lambda_0/\alpha\epsilon_{ss}\eta_0 = 5.4372 \times 10^{-10} \text{ m}. \quad \text{(B20)}$$

Note that a_{3D}/a(Si) = 1.0012. Since potential barrier is $\Delta\varphi_{03} = 1.22195$ V at $n = 3$ and $a_{3D} \approx a$(Si), therefore the silicon is the most suitable semiconductor material for observation of the quantum Schottky effect. Moreover, the plasmon oscillation mechanism of interaction between electrons (holes) allows the possibility to observe the quantum effects at room temperature and higher.

The formal determination of the quantum Schottky capacitance can be derived from the condition for quantization of velocity circulation[23]:

$$\omega_{Sc} S_{Sc} = h/m, \quad \text{(B21)}$$

where $\omega_{Sc} = 1/\rho_0 C_{Sc}$. Thus, the Schottky capacitance can be given by:

$$C_{Sc}/S_{Sc} = \epsilon_0/\lambda_0 = \pi(32/\epsilon_{ss}\eta_0)^2 C_B a_{3D}^{-2} \approx \epsilon_{ss} C_B a_{3D}^{-2}, \quad \text{(B22)}$$

where $\pi(32/\epsilon_{ss}\eta_0)^2/\epsilon_{ss} = 1.0038$ is considered. It is evident from the relationship (B22) that the Schottky capacitance C_{Sc} is the flat analogy of the spherical Bohr capacitance C_B. The minimal value of C_{Sc} will be at $S_{Sc} \to x_{03}^2$:

$$(C_{Sc})_{min} = \epsilon_0 \lambda_0^{-1} x_{03}^2 = 9\eta_0^3 C_B \pi^{-1} 2^{-8/3}. \quad \text{(B23)}$$

The maximum of C_{Sc} can be determined by the following way. Since the 1D energy density is the constant value:

$$\zeta_{03} = q\Delta\varphi_{03}/x_{03} = \pi\alpha^3 mc^2/(9\eta_0^{5/2} 2^{1/3}\lambda_0) = \text{const.}, \quad \text{(B24)}$$

therefore the fundamental mesascopic length (l_0) for the quantum Schottky effect can be defined as:

$$l_0 = 2W_q/\zeta_{03} = 9\eta_0^{5/2} 2^{4/3}\lambda_0 \pi^{-1}\alpha^{-3} = 3.7677 \times 10^{-4} \text{ m}, \quad \text{(B25)}$$

where $W_q = mc^2 = 511003$ eV is the rest energy of electron. Thus, the fundamental quantum area element for Schottky effect will be:

$$S_0 = l_0^2 = 1.4196 \times 10^{-7} \text{ m}^2. \quad \text{(B26)}$$

From the above it is evident that the quantum area element S_0 corresponds to the total rest energy of two electrons. The effective 2D resonant circuit of the quantum Schottky effect has the following reactive parameters:

$$\omega_0 = \hbar/mS_0 = 5123.9 \text{ rad/S} \quad \text{(B27a)}$$

$$C_0 = 1/\omega_0\rho_0 = 5.1805 \times 10^{-7} \text{ F} \quad \text{(B27b)}$$

$$L_0 = \rho_0/\omega_0 = 7.3524 \times 10^{-2} \text{ H} \quad \text{(B27c)}$$

for the angular frequency, capacitance and inductance, respectively.

We should point out that the value a_{3D} is close to the parameter $a_0 = (\lambda_0/\alpha)\sqrt{\epsilon_{ss}/\pi} = 5.4269 \times 10^{-10}$ m [a(Si)/a_0 = 1.0007] which has been obtained from the conditions: $\hbar\omega_s = W_B/\epsilon_{ss} = \alpha^2 mc^2/2\epsilon_{ss}$ and $\omega_s a_0^2 = \hbar/m$. Note that the energy of plasmon oscillation in that case will be:

$$\hbar\omega_{ps}(a_0) = \hbar\sqrt{q^2 N_{ss}/\epsilon_0\epsilon_{ss} m a_0} = 1.2231 \text{ eV},$$

the same as the Schottky potential barrier $q\varphi_{03}$ [$\hbar\omega_{ps}(a_0)/q\varphi_{03} = 1.0009$].